CERN/SPSC/75-24/P 45
March 5, 1975

AN EXTERNAL GAMMA RAY DETECTOR TO BE USED WITH BEBC WITH THE TST FOR EXPERIMENTS AT THE SPS(*)

A. Bettini(+), R. Bizzarri(¨), M. Bocciolini(°), E. Bressi(¨), E. Castelli(•), S. Centro(+), G. Ciapetti(¨), R. Conte(+), R. Contri(-), M. Cresti(+), M. De Giorgi(+), G. Di Caporiacco(°), R. George(×), M. Goldberg(×), B. Grossetete(*), I. Laakso(¨), F. Marzano(¨), M. Mazzucato(+), C. Omero(•), C. Ouannès(×), G. Parrini(°), D. Pascoli(+), L. Peruzzo(+), P. Proropat(•), V. Rossi(¨), G. Sartori(+), S.M. Sartori(+), M. Senè(×), M. Sessa(•), D. Teodoro(-), L. Ventura(+), D. Zanello(¨), G. Zumerle(+), T.P. Yiou(×).

Spokesman: D. Zanello - Roma.

(+) University and I.N.F.N., Padova
(¨) University and I.N.F.N., Roma
(°) University and I.N.F.N., Firenze
(•) University and I.N.F.N., Trieste
(-) University and I.N.F.N., Genova
(×) L.P.N.H.E. Université Paris VI
(*) Université Paris VII

(*) A preliminary version of this proposal has been presented in a letter of intention to the SPSC (CERN/SPSC/I 73-35).

1. INTRODUCTION

In the field of strong interactions the usefulness of the bubble chamber as a detector has been linked essentially to two main features:

a) 4π detection efficiency;

b) ability to analyze completely a large fraction of the final states produced by the interaction.

However, with the increase of the primary energy, feature b) gets progressively worse due to the growth of the average number of π^0's produced per event. In the range of energies that will be accessible to the new accelerators the fraction of 4C events will be less than 20% [1], while the 1C cathegory, due to accuracy problems, will become almost non-analyzable and, furthermore, will contaminate heavily the 4C channels[2].

The use of a downstream spectrometer to improve the measuring accuracy on the fast charged secondaries will at most gain a fraction of the 1C events.

On the other hand the use of a technique allowing the detection of γ-rays with good efficiency, can at the same time bring to negligible levels the contamination to the 4C channels, yield a clean sample of $1\pi^0$ events and allow with some efficiency the analysis of the multi-π^0 channels.

This last point is something completely new in the field of the hydrogen bubble chambers.

In order to maintain features a) and b), one should be able to detect γ's with high efficiency over the entire solid angle and to measure the π^0 momentum with an accuracy comparable to the one for charged tracks.

The possible methods to obtain γ-detection in a hydrogen bubble chamber have been extensively analyzed by a TCC-working party [1].

The result of this study indicates as the best solution the use of a hydrogen track-sensitive target (TST) surrounded by a high Z mixture ($Ne-H_2$).

This technique has already been successfully experimented at Rutherford Lab. [3]. At present a TST is being installed in the 12 foot Argonne chamber [4] showing the feasibility of this technique even in chambers the size of BEBC.

However, at SPS energies this technique will have severe problems for the π^0's emitted in the forward cone. The solution

of using a truncated target to detect these π^0's in the high Z liquid, will impose severe constraints on the number of events per picture, due to the confusion in the forward region of the chamber [5] and in any case the accuracy in momentum measurement of the fast π^0's won't be matched by the accuracy for the fast charged tracks (see Sect. 3).

A valid alternative is to give up the detection of the forward going π^0's in the chamber (using a wall to wall TST) and to use an external γ-detector to cover the solid angle not seen in the chamber.

CERN is planning to build a TST for BEBC to be used for experiments at SPS energies. Tests of this target will be carried out during the 1975 West Hall shut down, and the first use of the TST for hadronic experiments is foreseen for 1978-79.

We propose to build an external γ-detector (FGD) to be used in connection with the TST and to be ready around 1978.

This FGD together with the external-particle-identifier (EPI) [+] which is now under construction at CERN [6], would be general facilities attached to BEBC to carry on hadronic physics at SPS energies.

Since the FGD is usable even in connection with other devices (like a rapid-cycling-bubble chamber), it is not unconceivable that during the long neutrino runs it could be attached to other experiments.

Keeping in mind that the FGD is a "general facility" type of instrument we are not going to indicate any specific experiment it will be used with.

As far as can be seen now the study of strong interaction dynamics at SPS energies will move along two main lines of approach: inclusive type studies and multiparticle final-state analysis. In both cases π^0 detection will be of great use yielding the neutral multiplicity behaviour as function of energy, single π^0 inclusive cross sections, π^0-π^0 and π^0-charged particle correlations and giving the only way of access to high multiplicity channels, which will certainly contain several π^0's.

We may remind that many of the letters of intention and several

---

[+] The EPI will help to identify the fast charged particles. It is highly desirable that the two instruments run together in order to provide as complete an information as possible for

of the proposals for experiments with BEBC presented to the SPSC make explicit reference to the use of a TST and a FGD. To these proposals we refer for details on the physics motivations for the detection of neutrals.

Moreover, and if one takes also into account the fact that FNAL is already working in this energy range, it is difficult to know four years ahead of time which experiments will be the most interesting in 1978. For example, it is not unconceivable that the new long lived particles that are being discovered now may shift the interest to areas where a bubble chamber equipped with detectors of electromagnetically interacting particles may be very useful.

In Sect. 2 we will describe the apparatus we propose to build, in Sect. 3 we will discuss its performance and some problems it will meet, and finally in Sect. 4 we will present a cost estimate and a construction schedule.

2. DESCRIPTION OF THE APPARATUS

Although the gamma detector we are considering could be used to convert and measure gammas coming from interactions produced in any target and could be used in association with many types of experimental apparatus (rapid cycling bubble chambers, streamers, spectrometers) we shall taylor the design to BEBC with a TST.

The size of the apparatus is fairly well determined by the following conditions:

1) the apparatus should be placed behind the EPI, which means approximately 20 m from the BEBC center (see Fig. 1).
2) The apparatus should be matched to the TST size and shape. This is assumed to be 360x60x10 cm^3 (not tapered(+)). The vertical size (10 cm) is defined by the request for the slow charged tracks to have at least 5 cm length in hydrogen for sufficient direction determination accuracy.. Moreover, it is not desirable to make this dimension larger since one of the major sources of losses for the FGD is the γ conversion in the exity window of BEBC and it doesn's

---

(+) The use of a tapered target, as suggested in Ref. 5, doesn't seem to give any improvement to the performance

seem realistic to reduce the window thickness over a region wider than 10 cm in the z-direction.

Under these conditions the dimension of the FGD in the z-direction is determined to be about 100 cm, corresponding to an angular acceptance of ±25 mrad. Requiring the same angular acceptance in the y direction and taking into account that the beam will be spread over 40-50 cm one ends up with about 150 cm for the lateral size of the detector. The solid angle covered by the detector will therefore be $3.8\ 10^{-3}$ sterad.

It will be shown in Section 3 that with these dimensions the efficiency of the apparatus is sufficiently high.

The components of the apparatus are again rather well determined by the condition that momentum and angular precision for a π° be matched to the precision for a charged π of the same momentum.

1) Good energy resolution at all energies rules out a lead-scintillator sandwich detector. Indeed to achieve the energy resolution we need with a lead-scintillator sandwich we would have to use such a large number of very thin converter plates that the construction would become expensive and complicated and the operation difficult and less reliable. On the other hand NaI crystals are too costly and their response time too long. The use of lead-glass Cerenkov counters is therefore the only good solution.
2) Good angular resolution cannot be achieved with total absorption lead-glass blocks. Hence we need a vertex detector (VD) capable to localize the shower origin within few millimeters. With such VD-precision the standard lateral size of the LGC (15x15 cm^2) is adequate to our purposes.

The FGD then consists of two separate pieces, a counter hodoscope to detect the vertices of the showers and an array of lead glass Cerenkov counters to measure their energy.

In addition, some proportional wire chambers will be placed in the beam before it enters BEBC. Some more chambers will be placed right after the exit window and as close to it as possible. The operation scheme of the FGD is the following.

The chambers in the beam detect the primaries, recording their coordinates and labeling them with ordinal numbers, according to the time of their arrival. In this way we can associate each interaction in BEBC with the primary that produced

detected in the FGD the information is stored on analog buffers whose contents are associated to the ordinal number of the primary that produced it. In this way we can associate the showers to the interactions in BEBC. The input to the buffers is then inhibited and the PM's outputs are switched onto another set of buffers.

This switching operation will take place in 20-30 ns. The gate length in order to perform the integration of the PM signal is expected to be of the order of 100-150 nsec. With 3-4 interactions per picture and a spill time of 5-6 μsec (the length of the RF cavities pulse) the probability of a second interaction in the same gate is about 2%. To each PM we can connect in succession 4 different buffers, so that, for each BEBC picture we can record the information relative to a maximum of 4 γ-producing interactions. At the end of the SPS burst the contents of the buffers are read into the computer memory.

A detailed description of the various parts of the FGD and of its operation follows.

a) The hodoscope.

It consists of a stack of 9 plates of converter 1.05x1.50 m^2 for a total of 4 to 6 radiation lengths interlaced with 9 layers of finger counters 1 cm thick arranged along three directions. All the counters for a given coordinate are viewed by the same photomultiplier so that the vertex detector gives for the shower only one set of coordinates, sampling, however, each coordinate at three points along the axis of the shower with comparable precision for all three coordinates.

The height of the pulses will be measured and this will allow the determination of the shower vertex with an accuracy of a few mm , by determining the center of gravity of the signals of adjacent counters [7,8], and moreover will give a measurement of the fraction of the energy lost by the photon before the LGC. This loss will depend on the energy of the photon [9]: for a 10 GeV/c gamma it should be of the order of 10%, so that a measurement with a (10-20)% accuracy will match the few percent accuracy of the LGC.

The lateral size of the finger counters will be chosen between 1.2 and 1.5 cm. In this way the positional error will

tically the uncertainty arising from the correlation of the frame of reference used for the BEBC pictures to the external frame of reference and which might well be of the same order of magnitude. Tests will be made by CERN with wire chambers placed before and after BEBC, to determine this correlation (CERN/D.Ph.II/Beam 74-6) so more will be known about it by the time the FGD will be ready. The wire chambers that will be placed in the beam and right after the BEBC exit window will help reduce this uncertainty.
The final choice of the lateral size and of the orientation of the three coordinates will be made in such a way to get the best compromise between the numbers of PM's to be used and the length of the finger counters.
Assuming a configuration where x is horizontal and u and v are at 60° with respect to x and to each other we get a total of 310 PM's with a counter size of 1.5 cm and 388 PM's with a size of 1.2 cm. The maximum length for the finger counters is 1.5 m.
A simple procedure like the one adopted in Ref. 8 should permit to have essentially uniform response along the finger and thus avoid the problem of calibrating the absorption coefficient of the counters.

b) *The Lead-Glass Cerenkov counters.*

The array will consists of 70 glass blocks 15x15x60 cm^3 equivalent to 24 radiation lengths, capable of absorbing almost completely (95%) photons of energies up to 35 GeV. The counters will be viewed by 5" PM's like the EMI 9530K. The LGC give an accuracy on the measurement of the photon energy

$$\frac{\Delta E}{E} = \pm \frac{.05}{\sqrt{E}} \qquad \text{with E in GeV}$$

with a plateau at 1%.
We plan to calibrate each block using high energy electron beams. To monitor the stability of each counter during normal operation we envisage to use both light pulses from LEDS (light emitting diodes) and nuclear light sources like the one from NaI-Tℓ scintillator doped with Am^{241}.

c) The read-out system.

Since we are interested in measuring the energy deposited in the LGC and in the VD we must record the pulse area of the signals of each PM. This will be done on capacitive buffers (allowing 4 buffers per picture, following an idea similar to the one to be adopted in the ISIS system [10]). After the burst the analog signals will be converted into 12 bit digital information to be stored in the computer.

The A/D conversion will supply, on the 12 bits, a resolution of better than 1 part in a 100 over an energy range from 1 to 100 GeV. In Appendix III, we present a tentative scheme for the read-out electronics. Tests are being made on a prototype and preliminary results are satisfactory. The entire read out system and the control electronics (high-voltage controls, calibration checks, etc...) will be built according to CAMAC standards.

The system will be linked to a computer with a CAMAC branch-driver controlling up to seven crates.

d) The trigger.

Although no trigger is used for the interactions in BEBC, a trigger is needed for the FGD, lest the first four primaries cause the switching of all the buffers even if they are all empty.

Such a trigger should cause switching of all the buffers every time at least one photon enters the apparatus.

In principle a trigger ought to be designed specifically for each experiment. However, one must keep in mind that since pictures in BEBC will be taken anyway, the trigger needn't be too selective.

A number of such non selective triggers can be conceived, like for instance:

I) disappearance of the primary, taking advantage of the good angular collimation of the BEBC beam;

II) appearance of a shower signal on a counter placed behind the VD;

III) multiplicity selection in the wire chambers or in a counter hodoscope placed behind the window.

3. THE PERFORMANCE OF THE APPARATUS

We shall discuss in this Section the performance of the apparatus we intend to build, namely its efficiency for π^0 detection and its measurement accuracy.

a) Efficiency.

In order to determine the efficiency of the apparatus we have carried out Montacarlo calculations taking into account the performance of the two parts of the compound system (CBS), i.e. the chamber and the FGD, and allowing for the presence of the exit window and the EPI.

At present a photon produced in BEBC will cross before entering the FGD, 0.5 cm of steel of the BEBC exit window, plus 0.5 cm of steel of the vacuum tank window. The second window can, without any problem, be replaced by a much thinner one, a few mm of Al.

For the first run of the FGD, we shall have then to consider that the γ's will cross 0.5 cm of steel before being detected by the FGD. It is conceivable that for successive runs the exit window thickness may be reduced over a region of 10x60 cm^2. Safety reasons put a lower limit probably at .2-.3 cm.

A detailed discussion of the results of the Montecarlo with 0.2 cm window, is given in the Appendix I, together with the description of the relevant geometrical parameters defining the compound system.

We stress that the presence of the FGD is crucial for the π^0's emitted in the forward cone. In fact, as can be seen from Fig. 4, which gives the π^0detection efficiency as function of the Feynman variable x (for more details see Appendix I) the efficiency of the chamber alone, which is very good in the backward cone, drops rapidly to zero around x=0.

The efficiency of the FGD is rather flat as a function of x for x>0. Its value is around 60% for a window thickness of .2 cm and around 50% with .5 cm. The losses are due to: geometrical inefficiency $\sim$20%; conversion in the EPI frame $\sim$10%; conversion in the window (8-19)% depending on the thickness.

Both the window and the EPI frame will be a source of spurious γ's coming from the bremsstrahlung of electron pairs. Moreover spurious γ's may be produced by the interaction of secondary charged particles.

For what concerns the exit window, with a thickness of .5 cm, about 75% of the converted γ's will produce a bremsstrahlung γ with an energy higher than 100 MeV. Most of these γ's will hit the FGD.

This difficulty can be overcome by placing a telescope of small wire chambers (10x60 cm^2) as close as possible to the bubble chamber body. These cahmbers will detect the presence of an electron pair and allow the rejection of these events. With a thickness of .2 cm only 4% of the γ's crossing the window will produce secondary γ's. At this level the MWPC's would be probably unnecessary.

In a similar way a lead scintillator sandwich placed in front of the EPI and covering its frame will detect γ's hitting the frame itself and allow the rejection of these events.

For what concerns the amount of background coming from charged secondary particle interactions (not taken into account in the previous determination of the efficiency), this can be estimated to be of the order of few percent.

Finally, we remark that the fraction of events having a charged particle hitting the FGD together with some γ's is less than 10 % and the separation is large enough to avoid confusion (see Appendix I).

b) Accuracy.

In Fig. 8 a) and b) we show $\frac{\Delta p}{p}$ and $\Delta\theta$ as functions of energy for charged tracks (measured in hydrogen), for π^o's measured inside the chambers (2 γ's converted in the mixture) and for π^o's measured in the FGD (2 γ's converted in the FGD). The dotted line indicates the contribution of the multiple scattering error for the charged tracks measured in the Ne-H_2 mixture.

For full details on the formulae used on the assumptions made in order to compute these errors see Appendix II.

For what concerns $\Delta p/p$ it can be seen that for π^o's measured in the chamber the accuracy is certainly worse than that for charged tracks. As the energy grows this mismatch increases (+). This is a strong argument against the use of a truncated target.

(+) Furthermore, the momentum accuracy on fast charged secondaries will be improved by using the MWPC's placed in front and in

For the π^o's detected in the FGD the situation is much better: around 15 GeV/c the accuracy on the π^o's becomes equal to the one on the charged tracks and then improves.

Moreover, from our Montecarlo calculations we know that at 50 GeV/c primary energy, the spectrum of the π^o's detected in the FGD begins essentially at 5 GeV/c.

For $\Delta\theta$ it can be seen that even the angular accuracy of the FGD is well matched to the one on charged tracks.

Since the π^o mass resolution depends mainly on the accuracy on the γ's direction at all energies, this resolution is very good even if both γ's are measured inside the chamber (FWHM $\simeq$ 30 MeV). The resolution when both γ's are seen in the FGD is comparable if the γ's conversion points are measured with an accuracy of about 5-6 mm.

In Fig. 9 a) and b), we present the π^o-π^o mass resolution (at a primary energy of 50 GeV/c) in two different mass regions for the compound system.

In Fig. 10 a) and b) we show the average resolution in the x(Feynman) variable and in the rapidity y.

For what concerns the pairing efficiency, this will be certainly very good [5]. Our estimate for a $2\pi^o$ channel with 4 γ's converted is better than 90%.

c) Miscellanea.

The FGD will probably sit on the same platform as the EPI. This should then be extended by 2÷3 meters behind the EPI. The EMI that will surround BEBC should be foreseen with a removable central module in order to have a free path for charged or neutral secondaries, when BEBC is running for hadronic experiments. It might be possible then to design the platform for the EPI-FGD in s ch a way as to make it possible to move the apparatus 4m towards BEBC, to occupy the space freed by the EMI module. In this way one would gain, for the FGD, 4m/20m, that is its angular acceptance would be increased by 20%.

4. SCHEDULE AND COSTS

a) Prototype.

A prototype is beeing built, consisting of 4 lead glass counters of dimension equal to those envisaged for the final set up ($15x15x60$ cm^3). In front of these a Vertex Detector covering an area of $30x30$ cm^2 will be placed, consisting of a scintillator-lead sandwich with the counters on two axes 30 cm long and the counters on the third axis 1 m long. The read out will be made with the buffers and switching circuits foreseen for the final design.

We intend to perform the following tests:

I) calibration of the PM response vs the shower energy;
II) determination of the light attenuation in the finger counters;
III) determination of the accuracy on the measurement of the position of the shower vertex as function of the thickness and number of the lead plates on the VD;
IV) tests of the operation of the fast buffering and switching of the PM's output.

This prototype will be ready in the Summer 1975 and will be then carried at CERN for a test on some test beam containing electrons.

After this first test it will be probably carried at FNAL to be used in an experiment with the 30" hybrid system on interactions of π^-, p, π^+ at 150 GeV/c (Exp. E-299).

Contacts in this sense have already been taken with Prof. I.A. Pless, spokesman for the experiment and with Fermilab. This second test will be made in conditions very similar (except for the read-out time available) to the actual operation with BEBC.

b) Final project.

The prototype construction and first test will enable us to define the final project, which should be ready at the end of 1975. The collaboration intends then to apply for its financing with the local authorities (French and Italian) and to submit it to CERN for its final approval.

Some of the general parameters of the apparatus can be fore

they may have for the integration and compatibility with the rest of the equipment.

1) The outside dimensions will be roughly:
   2.0 m horizontally;
   1.5 m vertically;
   2.0 m along the beam direction.

2) The total weight will be ∿8 tons. More than half of this weight is due to the lead glass array, which will be made in two separate pieces, so that each can be lifted independently by the 5 ton hydraulic crane that can operate while BEBC is full of H_2.

3) The FGD will be placed on the same platform as the EPI, which will move on rails set on the W.H. floor to adjust to different beam momenta. The FGD will then be equipped with an independent movement with respect to the EPI platform to perform the adjustment to the "neutral beam" line.

4) The FGD computer will be linked to the computers of the other facilities connected to BEBC.

c) Schedule and costs.

The prototype tests should answer essentially all the questions opened at present by the end of 1975. Construction of the FGD could then start at the beginning of 1976, and be finished by the end of 1977.

Although it is difficult to estimate, at present, the cost with any accuracy, due to the rapidly changing prices and to the uncertainty in the cost of some of the parts that are under development now, a tentative specification of the costs can be the following.

1)	Lead glass	600 KFs.
2)	PM's	280 "
3)	PM equipment (Power supplies, distributors, cables, μ-metal, etc.)	230 "
4)	Scintillators and light pipes	120 "
5)	Read-out electronics	364 "
6)	Trigger and fast electronics	128 "
7)	Monitor (LED, Am^{241} sources and electronics)	48 "
8)	Computer	340 "
9)	Racks, platform, etc.	280 "

6. CONCLUSIONS

We propose then, to build an external shower detector to measure forward π^0's produced in BEBC and not seen by the high Z liquid mixture surrounding the TST. The set up consisting of a lead-scintillator counter sandwich to detect the vertex of the shower and of a lead glass Cerenkov counter array to measure its energy will be ready by the beginning of 1978 and it will cost approximately 2.4 MSF. Its compatibility and integration with the other apparatus surrounding BEBC should pose no difficult problems and is being investigated now.

A prototype is being built at present and will be tested at CERN in the Summer 1975 and immediately afterwards will presumably be part of an experiment at FNAL with a bubble chamber in a 150 GeV/c beam.

The final design will be presented by the end of 1975.

Some work will be required of CERN in reducing the thickness of the material on the γ-ray path after BEBC exit window. This should be done also to accomodate wire chambers after the window.

These chambers will be very helpful also for tracing the emerging tracks to the EPI.

Some work should be done at CERN also to investigate the compatibility of the"hadron instruments" (EPI-FGD) on one side with the nutrino EMI on the other.

As a final remark, we remind that in our letter of intention we mentioned that a FGD like the one we plan to build can be used with detectors other than BEBC.

The collaboration is at present studying its use in conjunction with a rapid-cycling bubble-chamber, like, for instance, the one considered by the CERN-RHEL collaboration (see Ref. 12). A test of this possibility will be the use of the prototype in the experiment with the 30" hybrid system at FNAL.

Since the FGD will be a relatively compact and light piece of equipment, it should be possible to move it from the West Hall to the North Area and back without too many difficulties. Is is possible then, to imagine its use with one or the other instrument, according to the needs of particular experiments or when BEBC is used, for instance, for neutrino experiments.

APPENDIX I

Introduction

We present here some preliminary results on the efficiency of a "compound BEBC system" (CBS), consisting in a TST inside the chamber filled with a Ne-H_2 mixture plus an external detector for forward going γ's (FGD).

In the first section we describe the relevant geometrical parameters of the CBS; in the second section we present the result on the π^0 detection efficiency versus x (the Feynman inclusive variable) of the apparatus; in the third and fourth section we present some results on the π^0 detection for scaled high-energy events with one and two π^0's.

1. Geometrical parameters

In this section we list the geometrical parameters we have used throughout our computation.

In fig. 2 one can find the top view of the CBS at 50 GeV/c.

The beam direction has been defined assuming an angle of 108.5 mrad with respect to the north wall of the W.H. after the last bending magnet. This corresponds to having the average neutral axis (A.N.A.) roughly centered (over a primary momentum interval 50-150 GeV/c) with respect to the exit window of the chamber, assuming a fiducial volume of 270 cm.

The spread of the beam is $\pm$20 cm in the y-direction and $\pm$2.5 cm in the z-direction. The dip angle is zero.

The TST is a flat box, 10 cm in depth, 60 cm wide and with the axis parallel to the average beam direction at 50 GeV/c (in fig. 2 α=79 mrad).

The Ne-H_2 mixture radiation length has been taken to be 50 cm. Fig.3 shows the y-z section of the exit window and the iron thickness in the different regions,as we assumed it in our calculations.

The γ's going through the front-end of the TST see only 2 mm of iron. The vacuum tank window has been disregarded.

The FGD is positioned 20 m from the BEBC center perpendicularly to the ANA. The FGD is 150 cm wide and 100 cm high.

In our computations we have taken into account the effect of the EPI frame. This frame is parallel to the beam direction and starts at 12.5 m from the BEBC center and is displaced by 30 cm

with respect to the center of the beam position. Its dimensions are 10x100x800 cm^3.

For the BEBC magnetic field we have taken the last set of measurements both inside and outside the iron shielding, using only the z component. In particular the return field in the gap in the iron shielding is 20 Kgauss over 40 cm.

2. *Single π° efficiency*

In order to estimate the efficiency of the CBS for single π° detection, we have generated π°'s with the following criteria:

a) the x distribution is uniform between -1 and 1 ($x=p^*_{\pi^\circ}/p^*_{in}$);
b) the p_T^2 distribution is $e^{-5.7p_T^2}$ (corresponding to $\langle p_T\rangle$=.370 GeV/c);
c) we have taken these π°'s to come from interactions $p+p\to\pi^\circ+...$ with different primary energies (50, 75, 100, 150 GeV/c). The interaction point has been generated at random inside the fiducial volume and the direction of the incident proton at the interaction point has been obtained tracing completely the beam through the magnetic field.

We have generated 2000 events at each energy.

Fig. 4 shows the efficiency of the CBS as a function of x for events with both γ detected.

As can be seen, this efficiency is of the order of 70% for x<0, and 50% for x>0. In the forward region the main contribution to this efficiency comes from the FGD.

The drop of the efficiency for x>0 is due to the loss in the window (∿10%) and the presence of the EPI (∿10%).

Fig. 5 shows the efficiency for events with at least one γ converted.

The efficiency is remarkably flat and of the order of 90%.

3. *Scaled events with one π°*

We have used events of the type

$$\pi^+p \to p3\pi^+2\pi^-\pi^\circ \qquad (1)$$

scaled from 16 GeV/c up to 60 GeV/c, using the method cf C. Cecchet et al (maximum pionization hypothesis). The procedure for vertex generation is the same as in section 2.

A total of 1618 events has been processed.

In table 1 we present the number of events with both γ's and one γ converted and show they are distributed between the BC and the FGD.

TABLE 1

	2γ converted	1γ converted
In B.C.	830	148
In FGD	149	248
1 γ in BC -1γ in FGD	110	---
Total	1089	395

It can be seen from the table that the possible contamination to the $\pi^+p\rightarrow p3\pi^+2\pi^-$ process is 33% without FGD, but only 8% with the FGD.

Moreover the fraction of events (1) that give a 4c fit goes from 50% to 67% with the introduction of the FGD. There are 127 γ's that would be detected in the FGD but are lost because of the EPI.

Fig. 6 shows the energy distribution of the γ's converted in the BC and in the FGD.

Fig. 7 shows the distance between the centers of the two showers in the FGD generated by the events with both γ's detected in the FGD.

Assuming a lateral size of $\sim$15 cm for the high-energy showers (97% of energy deposited inside a cylinder of 15 cm diameter), we see that 85% of the γ-pairs are separated. However this situation grows worse as the energy increases.

The fraction of events where a charged particle hits the FGD together with some γ is 4%. (It grows with primary energy but it is less than 10% up to 150 GeV/c).

For these events the distributions of the distance between the γ and the charged particle at the FGD position is wide and flat, and there is only one event where this distance is less than 15 cm.

In the previous computation of the charged particle background in the FGD we have disregarded the effect of the EPI and the possible interaction of the secondary particles in the exit window.

However there are only two events where a γ is detected in the FGD and one charged particle hits the EPI.

As for the secondary particle interaction in the window, the average number of charged secondaries going through the window per interaction is two, and the interaction probability (assuming 2 mm thickness) is 1% .

4. $2\pi^\circ$ scaled events

The events of reaction (1) have been used also to produce $2\pi^\circ$ events, changing one π^- into a π° and the proton into a neutron.

A total of 1081 events have been processed. Table 2 shows the number of events with 4, 3, 2, 1 γ converted in the CBS and in the BC alone.

TABLE 2

	4γ conv.	3γ conv.	2γ conv.	1γ conv.	at least 1γ
CBS	538	362	148	29	1077
BC alone	303	249	358	116	1026

As can be seen from the table the possible contamination to the 4c process is almost the same for the BC alone and for the CBS and is less than 1%.

However the possible contamination to the 1c channel is 44% for the BC alone and 18% for the CBS.

We remark that in the "2γ converted" cathegory there are 89 events where the 2γ's detected come from the same π°. Hence the contamination to the 1c channel for the CBS could go down to 9%.

In addition to the distance between two γ's coming from the same π° (distance computed at the FGD for the γ's converted in it), we have considered the distance between γ's coming from

The fraction of events where there is a charged particle in the FGD together with some γ is 7%. Again the distribution of the distance between the charged particle and the γ is wide and f`at, and the fraction of events where this distance is less than 15 cm is less than 1%.

APPENDIX II

In order to estimate the errors on charged tracks we have used the standard three point error formulae (assuming zero dip tracks):

$$\left(\frac{\Delta p}{p}\right)_{meas} = 3.2 \times 10^{-4} \frac{\epsilon}{BL} p$$

with ϵ = setting error = 300μm
B = magnetic field = 35 Kgauss
L = track length = 1.8 m
p = momentum in GeV/c

$$\left(\frac{\Delta p}{p}\right)_{M.S.} = \frac{.16}{\beta B L^{\frac{1}{2}}} \qquad \text{assuming } X_{oH_2} = 9.9 \text{ m}$$

$$(\Delta\theta)_{meas} = \sqrt{26}\,\frac{\epsilon}{L} \times 10^{-6}$$

$$(\Delta\theta)_{M.S.} = 1.3 \times 10^{-3}\,\frac{\sqrt{L}}{p} .$$

For the Ne-H_2 mixture the M.S. errors must be multiplied by

$$\left(\frac{X_{oH_2}}{X_{o\ mixture}}\right)^{\frac{1}{2}} = 4.45$$

To estimate the errors on π^o's detected fully in the chamber the procedure is more lengthy. Firstly one needs to estimate errors on electron tracks and this brings in, besides the normal measurement and multiple scattering errors, also the Behr-Mittner term coming from Bremsstrahlung effects (1).

tracks to be measured. Assuming ([4]) $y_o = 0.3$ it does not seem feasible to use the optimal length, since the resulting bL value for high energy electrons is such that the fraction of measurable tracks would be too small.

Hence we have chosen a fixed length of 20 cm, which is already optimistic, since with this value only 60% of the electron tracks are measurable with the computed accuracy. With this choice we get

$$\left(\frac{\Delta p}{p}\right)^2 = 1.65 \times 10^{-3} p^2 + 10.8 \times 10^{-3}$$

with p in GeV/c.

Assuming now that the energy spectrum of the electron-positron pair is flat, the average configuration is the one where the γ-energy is shared in the ratio 1/4 to 3/4 by the two particles.

With this assumption the error on the γ-energy is on the average

$$\left(\frac{\Delta p}{p}\right)^2_\gamma = 1.03 \times 10^{-3} p_\gamma^2 + 6.75 \times 10^{-3} \qquad (1)$$

To evaluate the error on the π°, we make use now of the Trilling formula (Ref. 11):

$$\frac{\Delta p_o}{p_o} = \frac{\cos\theta^*}{\left[\left(\frac{p_1}{\Delta p_1}\right)^2 + \left(\frac{p_2}{\Delta p_2}\right)^2\right]^{\frac{1}{2}}}$$

where p_1 and p_2 are the γ-momenta and θ^* is the decay angle in the π° rest system.

Again taking into account that the average configuration is the one with $p_1 = 1/4\ p_o$ and $p_2 = 3/4\ p_o$ and using (1), after some algebra one obtains:

$$\left(\frac{\Delta p_o}{p_o}\right)^2 = \frac{9.3\times10^{-6} p_o^4 + 1.09\times10^{-3} p_o^2 + 11.4\times10^{-3}}{.64 p_o^2 + 13.5} \qquad (2)$$

Taking again trilling formula for the angular uncertainty $\Delta\theta$:

$$\Delta\theta = \frac{\sin\theta^{*}}{\left|\left(\frac{p_1}{\Delta p_1}\right)^2\left(\frac{p_2}{\Delta p_2}\right)^2\right|^{\frac{1}{2}}} \quad \frac{m}{p_o}$$

one obtains:

$$\Delta\theta^2 = \frac{5.5\times10^{-2}}{p_o^2} \times \left(\frac{\Delta p_o}{p_o}\right)^2 \qquad (3)$$

When the π^o is fully detected in the FGD we assume for the momentum error:

$$\frac{\Delta p_o}{p_o} = \frac{\pm 0.05}{\sqrt{p_o}}$$

since the chance that showers coming from γ's of different π^o's overlap is very small.

Showers coming from γ's of the same π^o will overlap more frequently and more so as the π^o energy increases. This will cause additional uncertainty in the knowledge of the energy of each of the two γ's, hence in the knowledge of the π^o direction.

However the vertex detector gives with a certain accuracy the position of the center of the two showers with respect to the lead-glass-pieces.

If one assumes to know the lateral energy distribution of the showers and that this distribution is weakly dependent on the energy it is possible to separate the two γ energies even when showers overlap.

We have carried out Montecarlo calculations assuming transversal energy distribution of the kind $e^{-r/L}$ and allowing for an uncertainty of ±5 mm in the knowledge of the center of the showers. The results of these calculations indicate that the main contribution to the angular uncertainty in the π^o direction comes from the uncertainty in the γ-vertices position. Therefore we calculated that the standard size of 15x15 cm^2 for the lead-glass-pieces is perfectly adequate. Because of the geometrical uncertainty in the relative position of the BEBC frame of reference and the FGD, we estimate that the minimum angular error for the π^o direction cannot go below 0.25 mrad.

APPENDIX III

Read out system

Th tentative circuit for data acquisition for every PM of the system is shown in fig. 11. The linear gate is made by transistors T1 to T6 following a rather classical scheme. When the circuit is ready for data acquisition, the bit A in the 4 bit shift register is set. The capacitor C_A is connected through CMOS gate G_A to the linear gate output and to the current generator I_p that keeps the capacitor charge constant until a gate signal arrives. The controlled current generator I_p provides to T5 a current higher than the current sunk by T1 (10 mA), allowing operation in linear region and at the same time a pedestal adjustable to few counts. As soon as a gate signal arrives the charge at the PM input is transferred to C_A. The trailing edge of the gate signal shifts bit A to B opening G_A and closing G_B storing the charge of C_A and leaving C_B ready for next signal. The next analog buffer is ready for a new acquisition in about 50 nsec after the end of the previous gate. (When the analog switch is open the leakage is about 10pC sec^{-1}).

At the end of the burst the current generator Ip is switched off and capacitors C_A to C_D are discharged in turn through the constant current I_C=10μA. The length of the output signals of the discriminator is proportional to the charges stored in the capacitors.

The discriminator outputs are then digitized in four 12 bit scalers. All the capacitors of each module are converted in four steps in a total time of about .8msec. At the end of the conversion the registers containing the digital data are read into the computer via DMA. It is also possible to transfer only significant data in less than 4 msec.

FIGURES

1) General layout of the EPI and the FGD behind BEBC.

2) CBS layout at 50 GeV/c primary energy.

3) A possible BEBC exit window with reduced thickness (y-z section).

4) π° detection efficiency of the CBS as function of x for the reaction $pp \to \pi^\circ + \ldots$ at several primary energies.
The continuous line gives the total efficiency for two γ's converted in the CBS.
The dotted line gives the contribution of the FGD when both γ's convert in it.

5) Efficiency of the CBS for at least one γ converted for the reaction $pp \to \pi^\circ + \ldots$ at several primary energies.

6) γ-energy spectra for γ's converted in a) BEBC and b) FGD for the reaction $\pi^+ p \to p 3\pi + 2\pi^- \pi^\circ$ at 60 GeV/c primary energy.

7) γ_1-γ_2 separation in the FGD for the reaction $\pi^+ p \to p 3\pi^+ 2\pi^- \pi^\circ$ at 60 GeV/c.

8) a) $\Delta p/p$ as function of energy.
b) $\Delta\theta$ as function of energy.
The continuous line is for charged tracks, the dashed line for π°'s fully detected in the mixture; the dash-dotted line for π°'s fully detected in the FGD.
The dotted line indicates the contribution of the multiple scattering error if the charged tracks were measured in the mixture.

9) a) π°-π° mass resolution for the reaction $\pi^+ p \to n 3\pi^+ \pi^- 2\pi^\circ$ at 60 GeV/c in the mass region $m_{\pi^\circ\pi^\circ} < 1.5$ GeV.
b) Same as a) in the mass region $m_{\pi^\circ\pi^\circ} \geq 1.5$ GeV.

10) a) Average resolution in the variable x for the reaction $pp \to \pi^\circ + \ldots$ at 50 GeV/c.
b) Average resolution in the variable y for the same reaction.

11) Scheme of the readout electronics.

REFERENCES

1) CERN/TCC 71-34 (1971), pag. 1.

2) CERN/ECFA 72-4 Vol. I (1972), pag. 31.

3) T.G. Coleman et al., NIM 107 (1973), pag. 399.
G.F. Ayres et al., NIM 107 (1973), pag. 131.

4) H. Leutz, CERN/ARGONNE.

5) CERN/ECFA 72-4 Vol. I (1972), pag. 13.

6) CERN/D. Ph. II Beam 74-5 (1974).

7) Yu. B. Bushmin et al., NIM 106 (1973), pag. 493.

8) A.V. Barnes et al., Preprint submitted to the London Conference (1974).

9) M. Holder et al., NIM 108 (1973), pag. 541.

10) C.B. Brooks (private communication).

11) G. Trilling, SLAC-5-E (1962), pag. 65.

12) CERN/SPSC 74-45, SPSC/T 14 (1974).

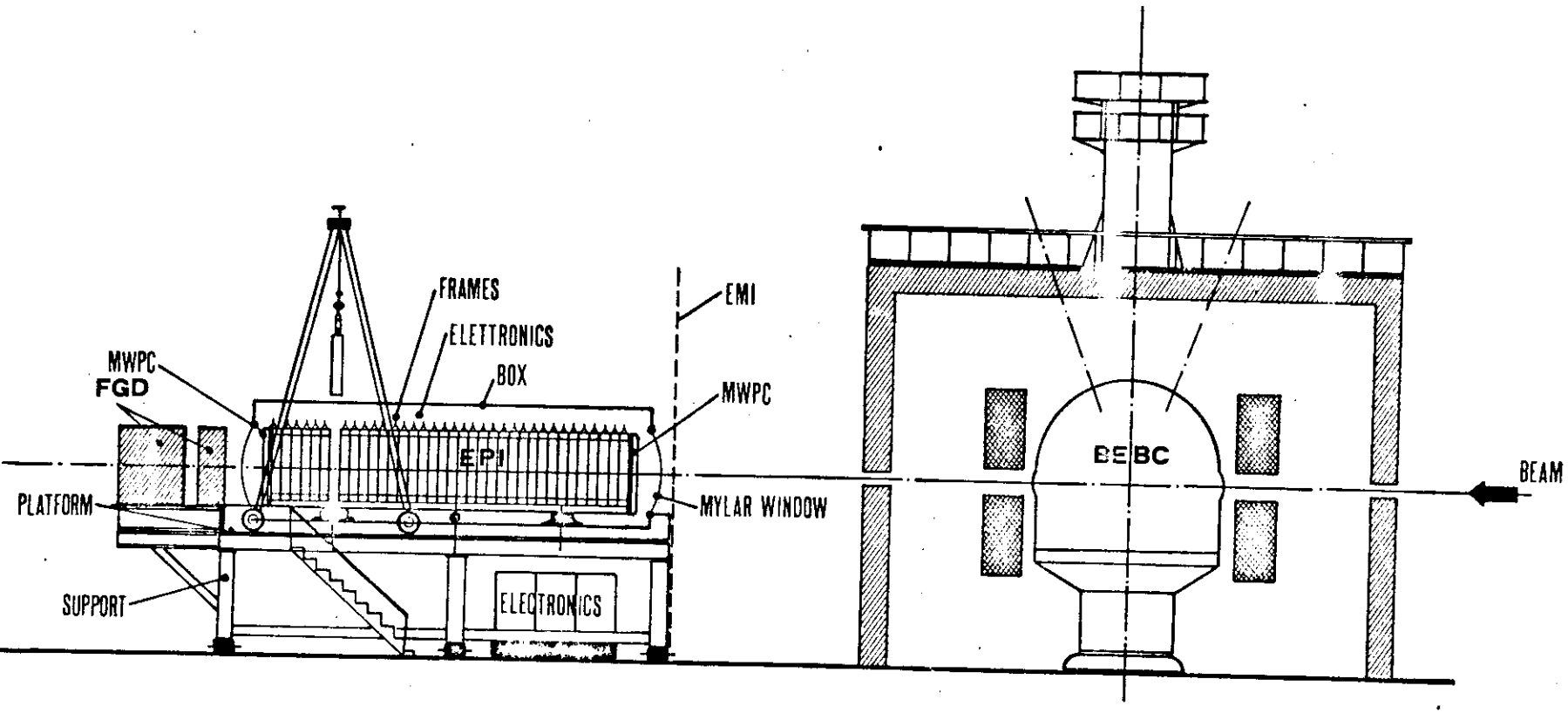
FRAMES
ELETTRONICS
BOX
EMI
MWPC
FGD
MWPC
EPI
BEBC
BEAM
PLATFORM
MYLAR WINDOW
SUPPORT
ELECTRONICS

FIG. 1

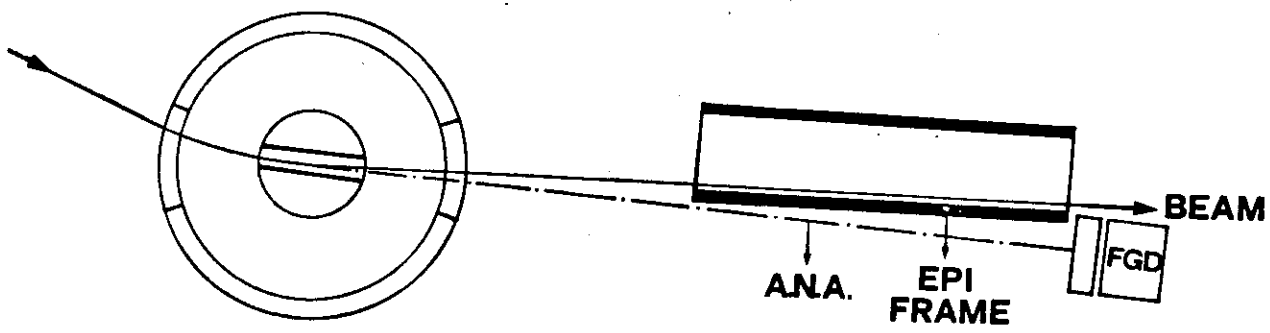

FIG. 2

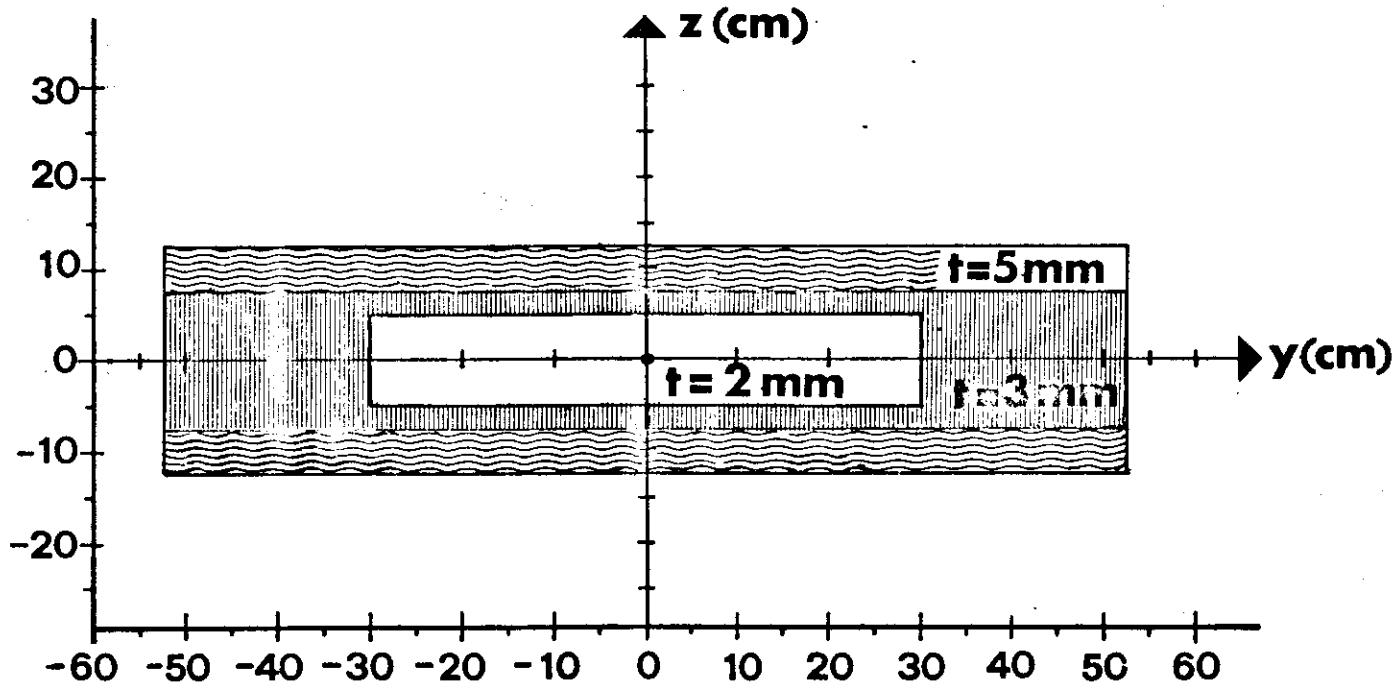
z (cm)
30
20
10
0
-10
-20
t=5mm
t = 2 mm
t=3mm
y(cm)
-60 -50 -40 -30 -20 -10 0 10 20 30 40 50 60

FIG. 3

FIG. 4

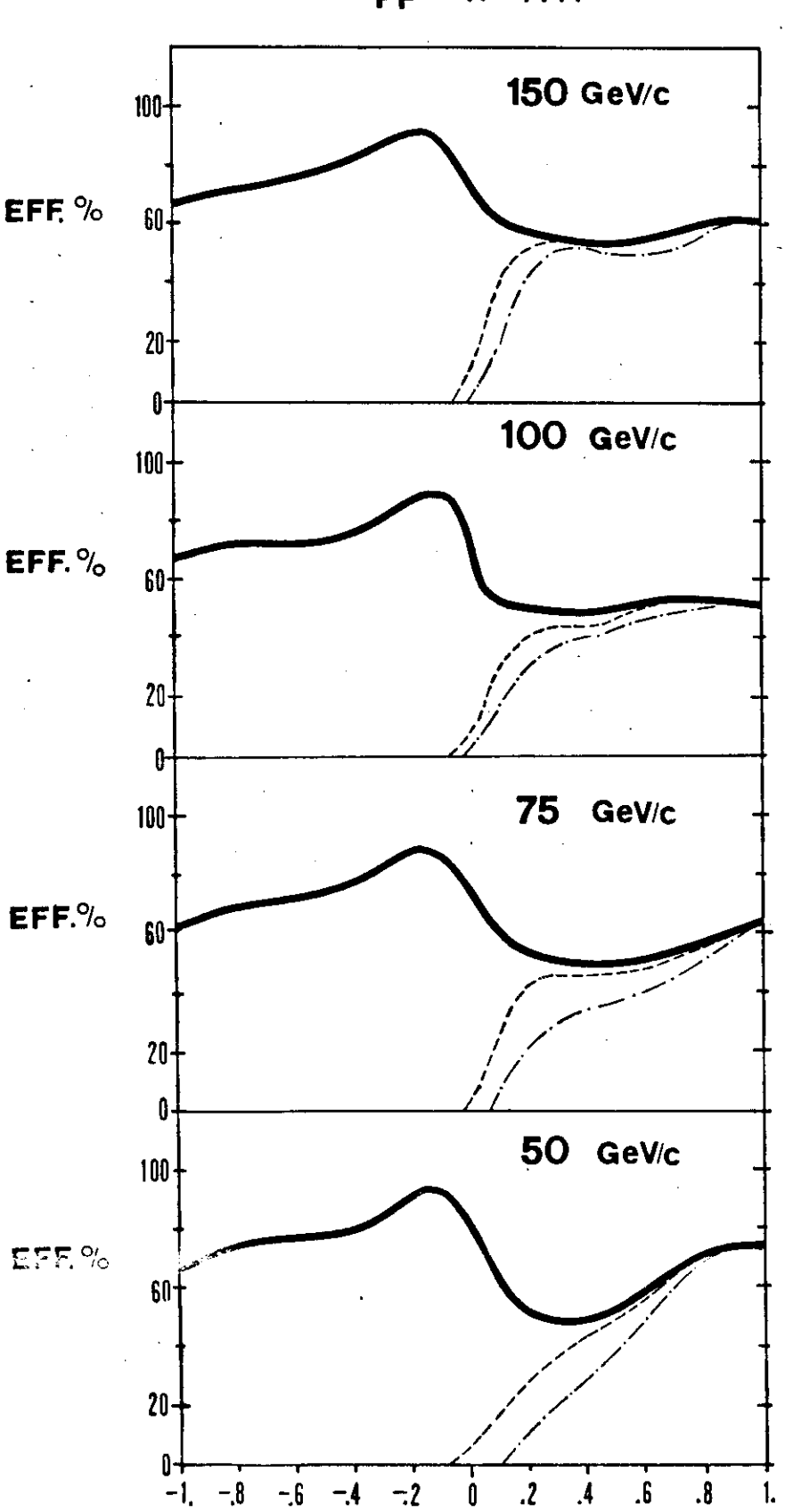
PP → π° + ...
150 GeV/c
100 GeV/c
75 GeV/c
50 GeV/c
EFF. %
100
60
20
0
-1.
-.8
-.6
-.4
-.2
0
.2
.4
.6
.8
1.

FIG. 5

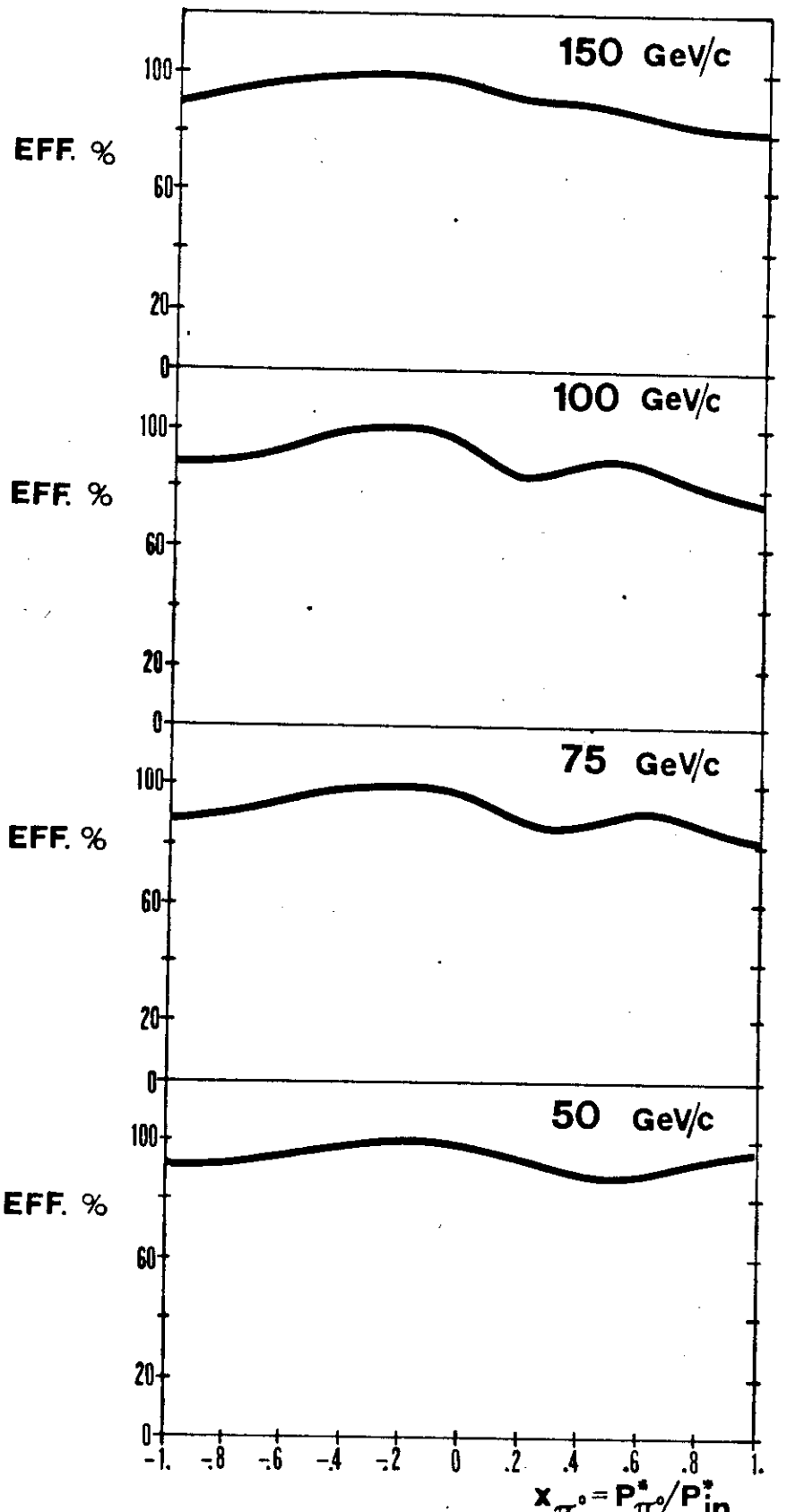
PP → π°+ ....
150 GeV/c
100 GeV/c
75 GeV/c
50 GeV/c
EFF. %
100
60
20
0
-1.
-.8
-.6
-.4
-.2
0
.2
.4
.6
.8
1.
$x_{\pi^0} = P^*_{\pi^0}/P^*_{in}$

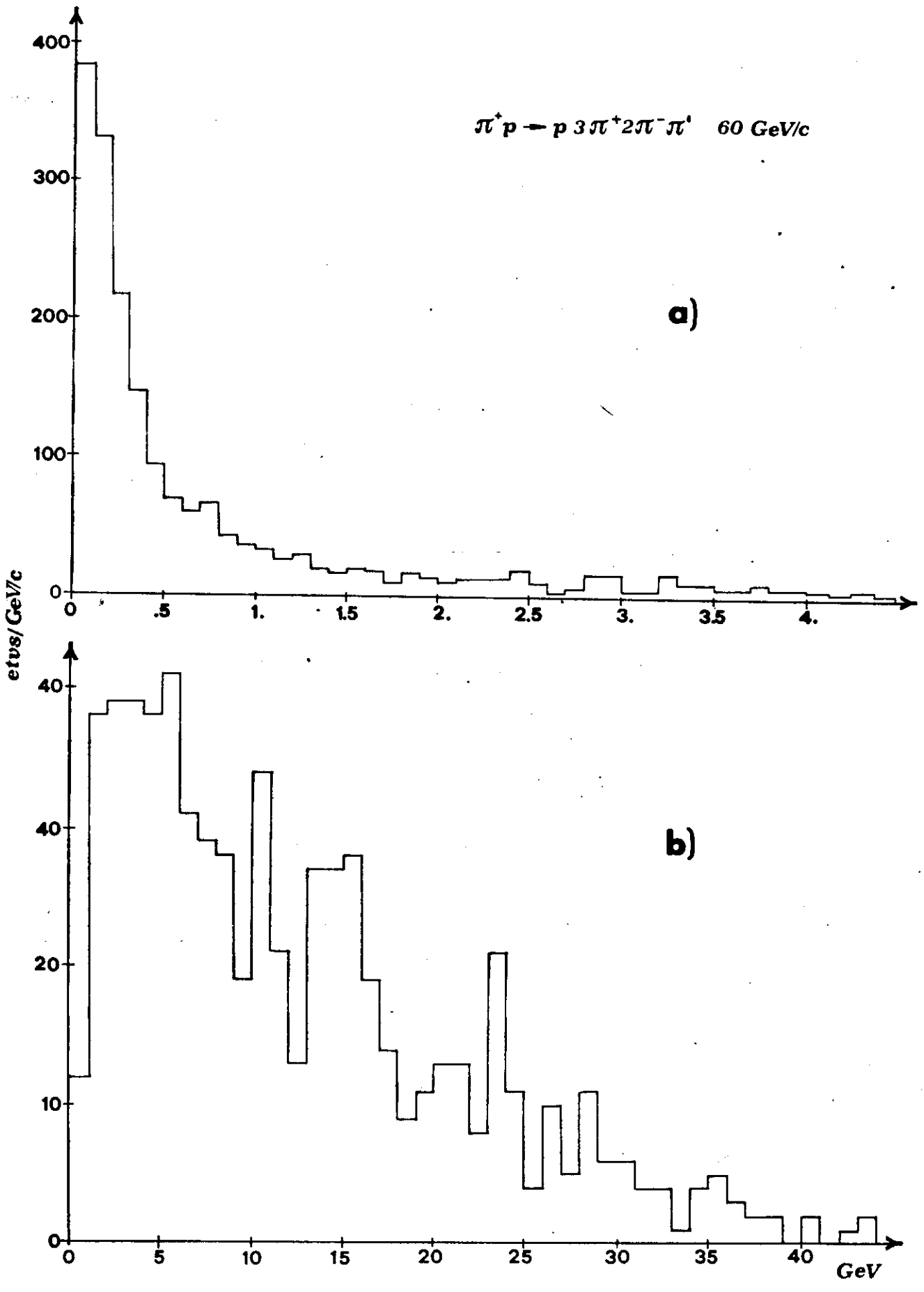
$\pi^+ p \rightarrow p\, 3\pi^+ 2\pi^- \pi^0$ 60 GeV/c
a)
b)
etvs/GeV/c
GeV
0
100
200
300
400
.5
1.
1.5
2.
2.5
3.
3.5
4.
10
20
40
5
15
25
30
35

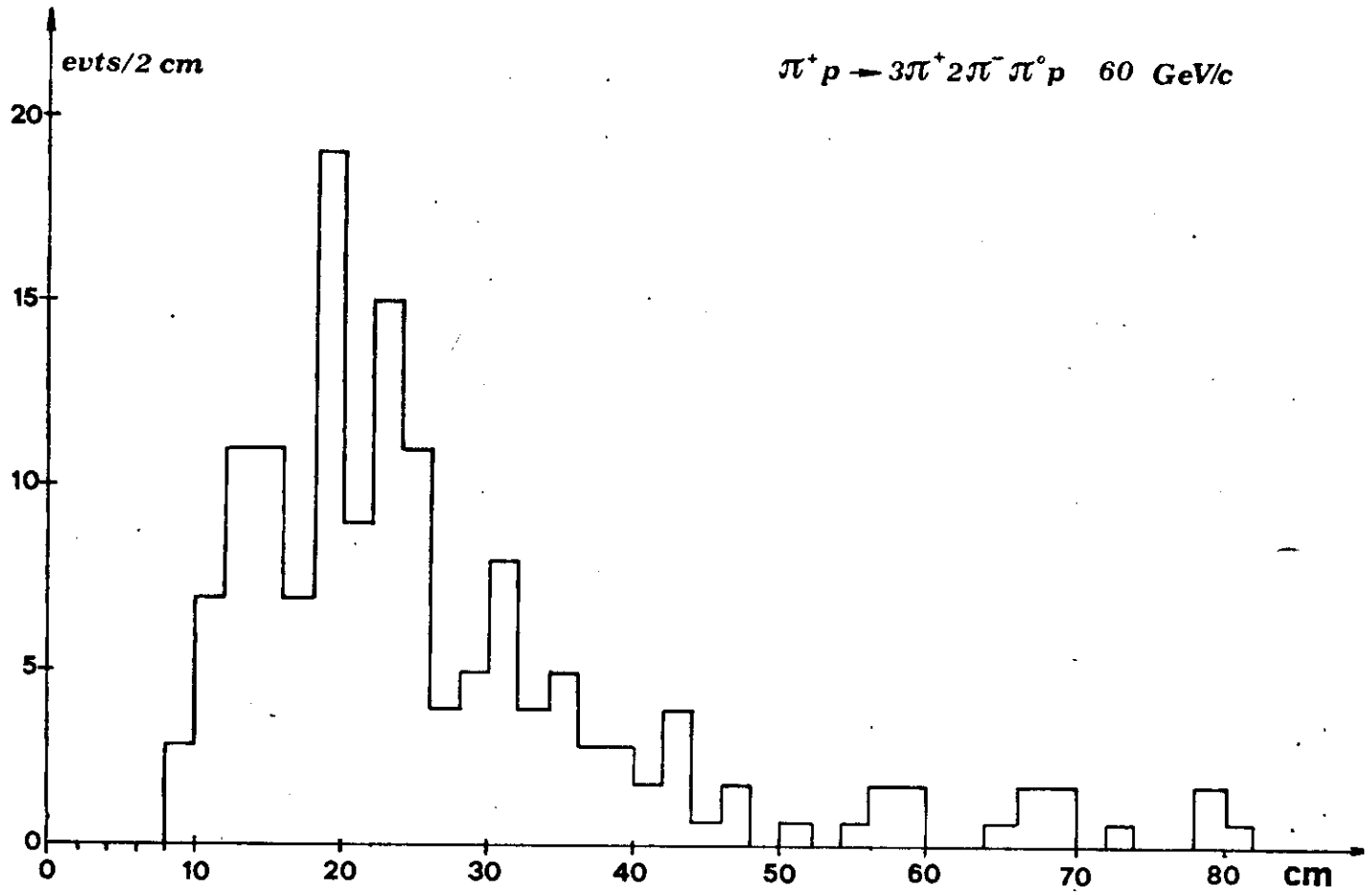
evts/2 cm
$\pi^+ p \rightarrow 3\pi^+ 2\pi^- \pi^\circ p$ 60 GeV/c
20
15
10
5
0
0
10
20
30
40
50
60
70
80
cm

FIG. 7

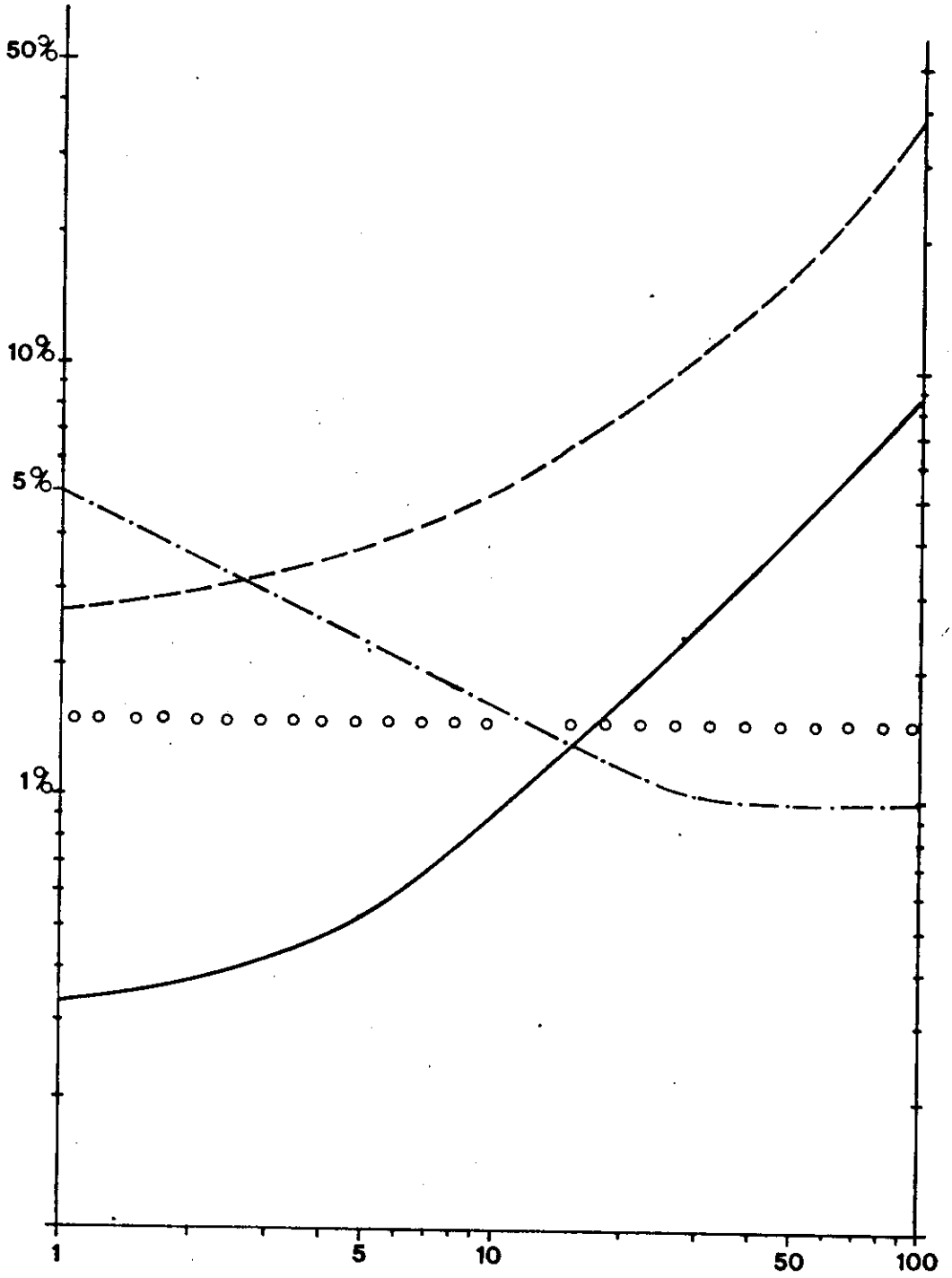

FIG. 8 a)

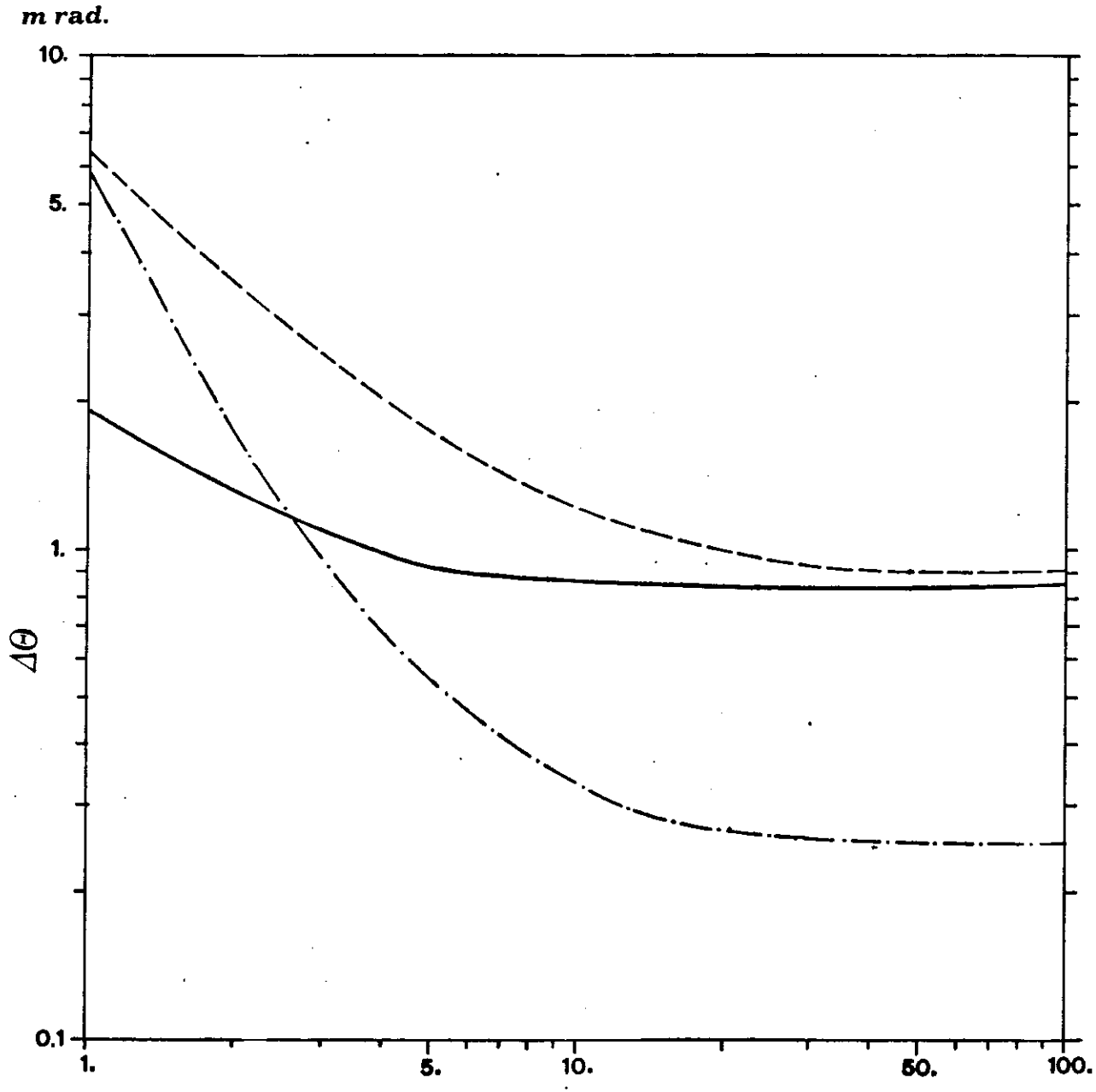

FIG. 8b)

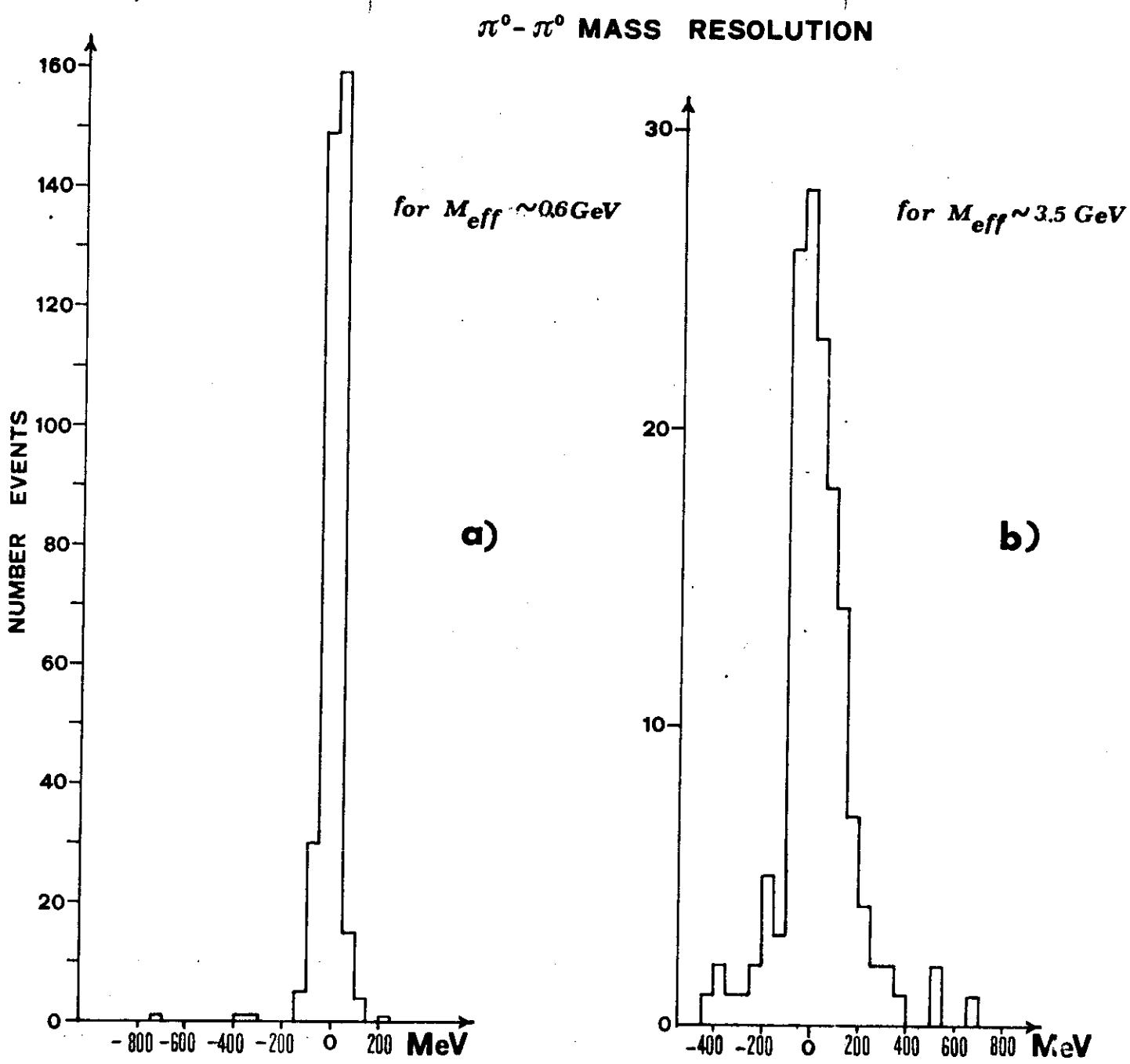
π^0-π^0 MASS RESOLUTION
NUMBER EVENTS
160
140
120
100
80
60
40
20
0
for M_{eff} ~0.6GeV
a)
-800 -600 -400 -200 0 200 MeV
30
20
10
0
for M_{eff} ~3.5 GeV
b)
-400 -200 0 200 400 600 800 MeV

FIG. 9

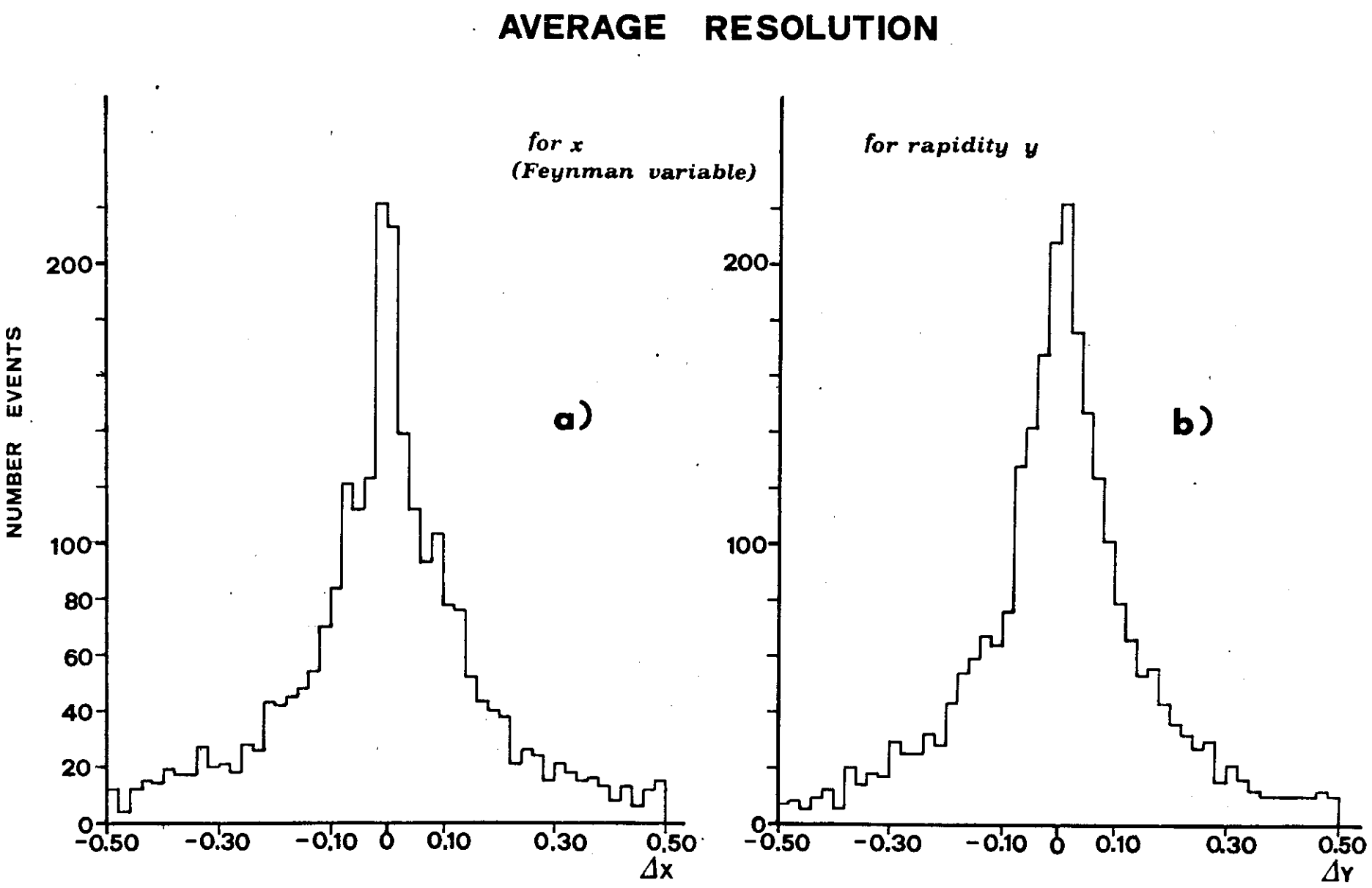
AVERAGE RESOLUTION
for x
(Feynman variable)
for rapidity y
NUMBER EVENTS
200
100
80
60
40
20
0
a)
b)
-0.50
-0.30
-0.10
0
0.10
0.30
0.50
Δx
Δy

FIG. 10

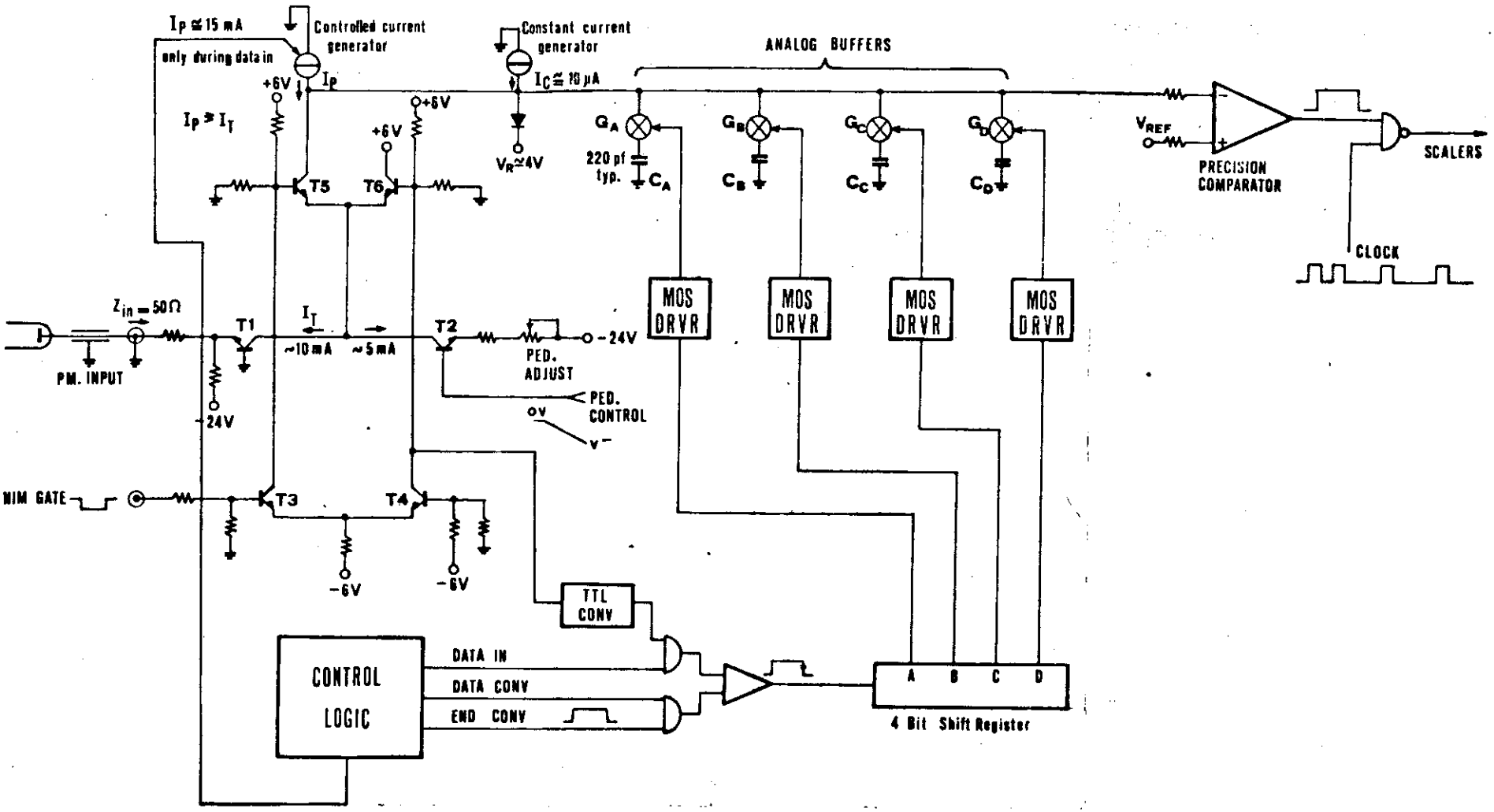
Ip ≅ 15 mA
only during data in
Controlled current generator
Constant current generator
ANALOG BUFFERS
+6V
Ip
Ip ≫ IT
+6V
+6V
IC ≅ 10 μA
VR ≅ 4V
220 pf typ.
GA
GB
GC
GD
CA
CB
CC
CD
VREF
PRECISION COMPARATOR
SCALERS
CLOCK
T5
T6
Zin = 50Ω
T1
IT
~10 mA
~5 mA
T2
-24V
PED. ADJUST
PED. CONTROL
0V
V-
PM. INPUT
-24V
MOS DRVR
MOS DRVR
MOS DRVR
MOS DRVR
NIM GATE
T3
T4
-6V
-6V
TTL CONV
CONTROL LOGIC
DATA IN
DATA CONV
END CONV
A
B
C
D
4 Bit Shift Register

FIG. 11